

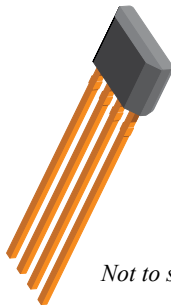
## Three-Wire True Zero-Speed Differential Peak-Detecting Sensor IC with Continuous Calibration

### FEATURES AND BENEFITS

- Unique design for robustness against high power EMC transients
- Peak detection based switching algorithm for large operating air gaps
- Minimum differential field 20 G<sub>pk-pk</sub>
- Running mode calibration for continuous optimization
- Precise duty cycle signal throughout operating temperature range
- Automatic Gain Control (AGC) for air-gap-independent switchpoints
- Automatic Offset Adjustment (AOA) for signal processing optimization
- True zero-speed operation
- Scan and IDDQ for increased test coverage

### PACKAGE:

4-pin SIP (suffix K)



Not to scale

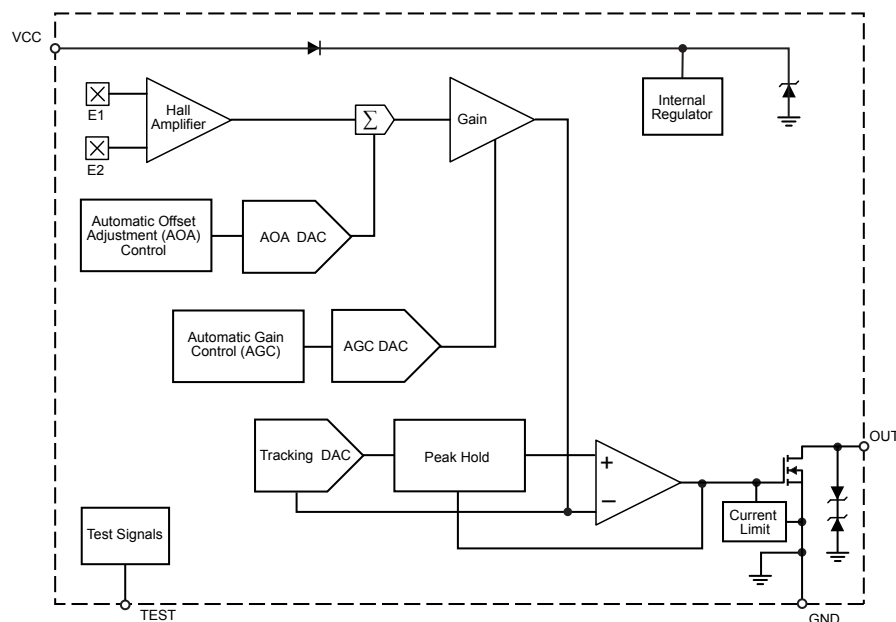
### DESCRIPTION

The A1469 is an optimized Hall effect sensing IC that provides a user-friendly solution for digital ring-magnet sensing, or when coupled with a magnet, ferromagnetic target sensing, in three-wire applications. The small device package can be easily assembled into applications for use in conjunction with a wide variety of target shapes and sizes.

The integrated circuit incorporates dual Hall effect elements with a 2.2 mm spacing and signal processing that switches in response to differential magnetic signals created by ring-magnet poles. The circuitry contains a sophisticated digital circuit to reduce system offsets, to calibrate the gain for air-gap-independent switchpoints, and to achieve true zero-speed operation. Signal optimization occurs at power-on through the combination of offset and gain adjust, and is maintained throughout the operating time with the use of a running-mode calibration. The running-mode calibration provides immunity to environmental effects such as micro-oscillations of the target or sudden air gap changes.

The device is ideally suited to obtaining speed and duty cycle information in ring-magnet-based speed, position, and timing applications, such as in speedometers.

The A1469 is available in a 4-pin SIP (suffix K) package. The package is lead (Pb) free, with 100% matte tin leadframe plating.



Functional Block Diagram

## SPECIFICATIONS

### Selection Guide

Part Number	Package	Packing*	Operating Ambient Temperature Range, $T_A$ (°C)
A1469LK-T	4-pin through hole SIP	Bulk, 500 pieces per bag	-40 to 150

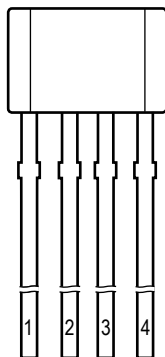


\*Contact Allegro™ for additional packing options.

### Absolute Maximum Ratings

Characteristic	Symbol	Notes	Rating	Unit
Forward Supply Voltage	$V_{CC}$	Refer to Power Derating Curves chart	28	V
Reverse Supply Voltage	$V_{RCC}$		-18	V
Output Current	$I_{OUT}$		30	mA
Reverse Output Current	$I_{ROUT}$		-50	mA
Reverse Output Voltage	$V_{ROUT}$		-0.5	V
Output Off Voltage	$V_{OUT}$		28	V
Operating Ambient Temperature	$T_A$	L temperature range	-40 to 150	°C
Maximum Junction Temperature	$T_J(max)$		165	°C
Storage Temperature	$T_{stg}$		-65 to 170	°C

### Pin-out Diagrams and Terminal List Table



Package K, 4-Pin SIP

### Terminal List Table

Name	Number	Function
VCC	1	Supply voltage
VOUT	2	Output
TEST	3	Test pin, float
GND	4	Ground

**OPERATING CHARACTERISTICS:** valid throughout operating voltage and ambient temperature ranges, typical data applies at  $V_{CC} = 12\text{ V}$  and  $T_A = 25^\circ\text{C}$ ; unless otherwise specified

Characteristics	Symbol	Test Conditions	Min.	Typ.	Max.	Unit <sup>1</sup>
<b>Electrical Characteristics</b>						
Supply Voltage <sup>2</sup>	$V_{CC}$	Operating, $T_J \leq 165^\circ\text{C}$	4	–	26.5	V
Undervoltage Lockout	$V_{CC(uv)}$	$V_{CC} = 0 \rightarrow V_{CC(\min)} + 1\text{ V}$ and $V_{CC(\min)} + 1\text{ V} \rightarrow 0\text{ V}$	–	–	$V_{CC(\min)}$	V
Supply Current	$I_{CC}$	$V_{CC} > V_{CC(\min)}$	3.0	5.0	7.5	mA
<b>Power-On Characteristics</b>						
Power-On State	POS	$V_{OUT}$ , connected as in figure 6	–	High	–	V
Power-On Time <sup>3</sup>	$t_{PO}$	$V_{CC} > V_{CC(\min)}$	–	–	2.3	ms
<b>Transient Protection Characteristics</b>						
Supply Zener Clamp Voltage	$V_{Z(\text{supply})}$	$I_{CC} = I_{CC(\max)} + 3\text{ mA}$ , $T_A = 25^\circ\text{C}$	28	–	–	V
Supply Zener Current	$I_{Z(\text{supply})}$	$V_{\text{supply}} = 28\text{ V}$	–	–	$I_{CC(\max)} + 3$	mA
Reverse Supply Current	$I_{RCC}$	$V_{RCC} = -18\text{ V}$ , $T_J < T_{J(\max)}$	–	–	–1	mA
Output Zener Clamp Voltage	$V_{Z(\text{output})}$	$I_{OUT} = 3\text{ mA}$ , $T_A = 25^\circ\text{C}$	28	–	–	V
Output Zener Current	$I_{Z(\text{output})}$	$V_{OUT} = 28\text{ V}$	–	–	3	mA
Output Current Limit	$I_{OUT(\text{lim})}$		30	–	85	mA
<b>Output Stage Characteristics</b>						
Output Saturation Voltage	$V_{OUT(\text{sat})}$	$I_{OUT(\text{sink})} = 20\text{ mA}$	–	220	400	mV
Output Leakage Current	$I_{OFF}$	$V_{OUT} = 24\text{ V}$ , output off	–	–	10	$\mu\text{A}$
Output Fall Time	$t_f$	$R_{PU} = 1\text{ k}\Omega$ , $V_{PU} = 20\text{ V}$ , $C_{OUT} = 10\text{ pF}$	–	2	–	$\mu\text{s}$
<b>Performance Characteristics</b>						
Operating Magnetic Signal Range	$B_{DIFF}$	Peak-to-peak of differential signal; operation within specification	20	–	1200	G
Operate Point <sup>4</sup>	$B_{OP}$	See figure 5	–	120	–	mV
			3	–	10	G
Release Point <sup>4</sup>	$B_{RP}$	See figure 5	–	120	–	mV
			3	–	10	G
Operating Frequency	$f_{OP}$		0	–	10	kHz
Analog Signal Bandwidth	BW	Equivalent to $f = -3\text{ dB}$	20	–	–	kHz
Initial Calibration Cycle <sup>5</sup>	$n_{cal}$	Output rising edges before calibration is completed, 0 offset, $f_{OP} \leq 200\text{ Hz}$	–	–	3	edge
Output Duty Cycle Precision	$D_{OUT}$	Using a pure sine magnetic signal, with $f_{OP}$ and $B_{DIFF}$ within specification	–	–	$\pm 15$	%
Output Period Precision	$T_{OUT}$	Using pure sine magnetic signal with $B_{DIFF} = 50\text{ G}_{pk-pk}$ and $f_{OP} = 1\text{ kHz}$	–	0.3	–	%
Allowable User Induced Differential Offset	$B_{DIFFEXT}$	Output switching only	–	–	$\pm 100$	G

<sup>1</sup> 1 G (gauss) = 0.1 mT (millitesla).

<sup>2</sup> Maximum voltage operation must not exceed maximum junction temperature. Refer to Power Derating Curves chart.

<sup>3</sup> Time required to initialize device. Power-On Time includes the time required to complete the internal automatic offset adjust. The DAC is then ready for peak acquisition.

<sup>4</sup> Values in G are based on device in maximum gain setting.

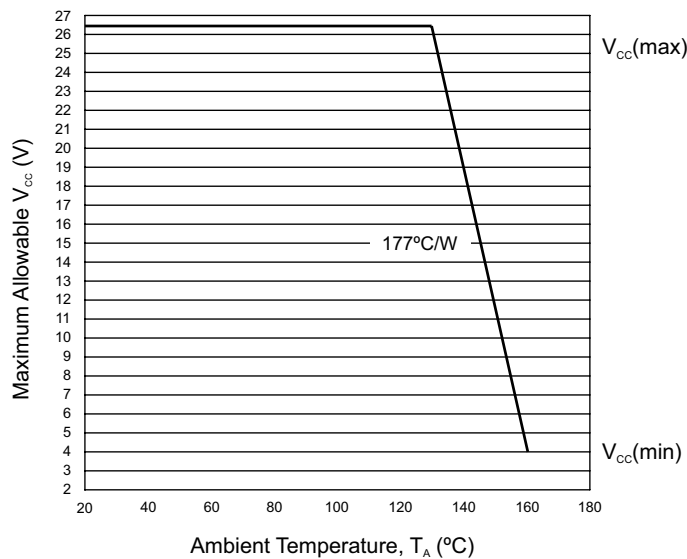
<sup>5</sup> Non-uniform magnetic profiles may require additional output pulses before calibration is complete.

Thermal Characteristics may require derating at maximum conditions, see application information

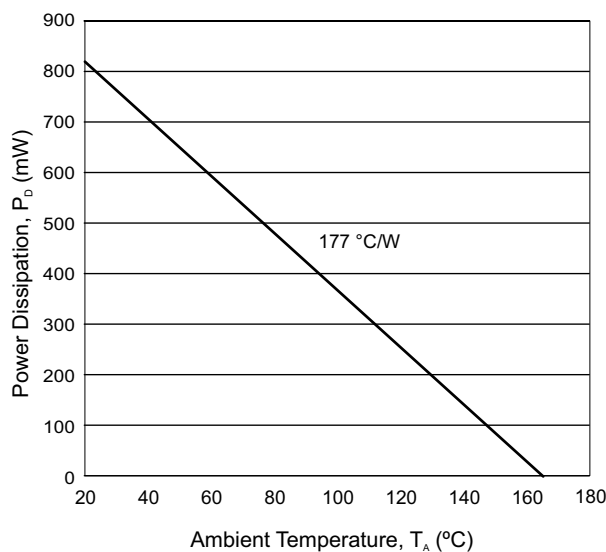
Characteristic	Symbol	Test Conditions*	Value	Unit
Package Thermal Resistance	$R_{\theta JA}$	On single-layer PCB with copper limited to solder pads	177	$^{\circ}C/W$

\*Additional thermal information available on the Allegro website.

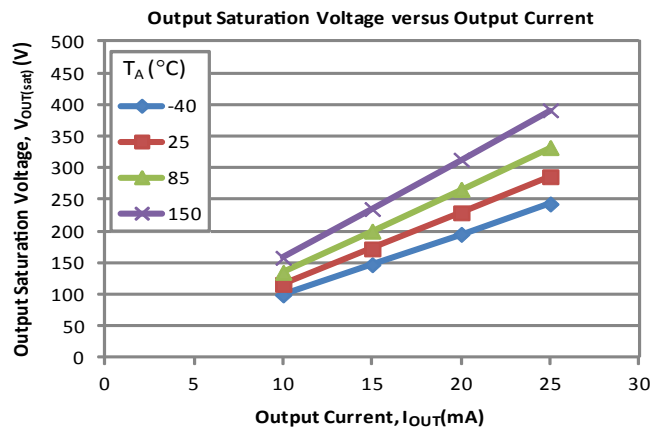
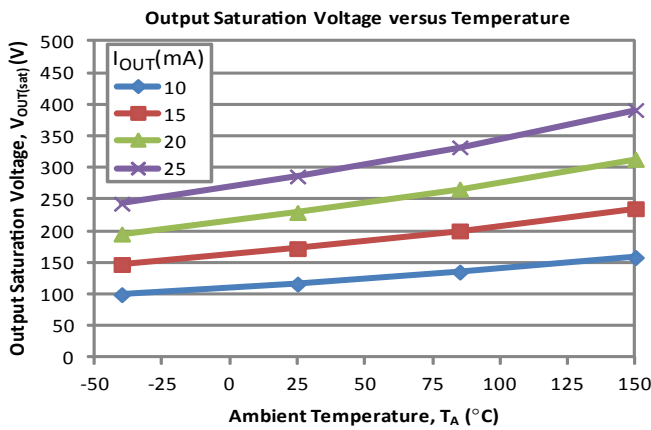
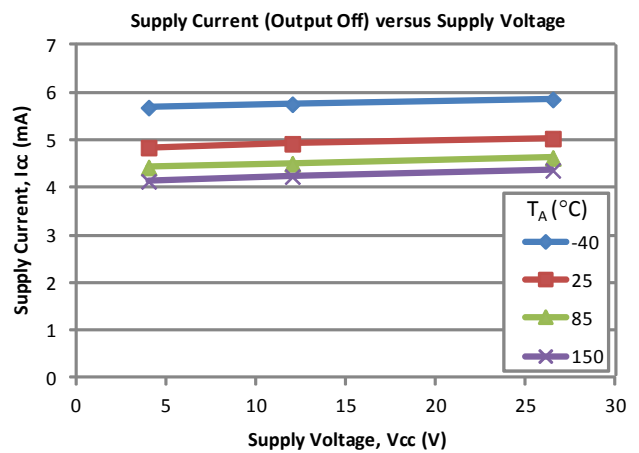
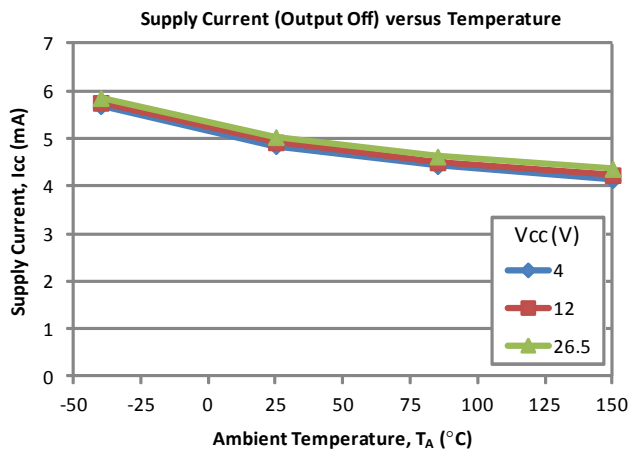
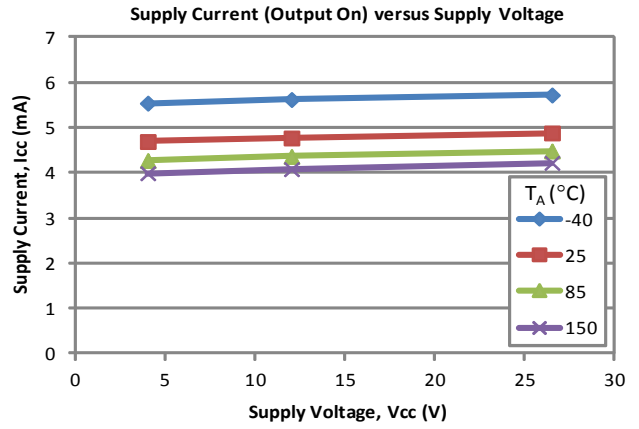
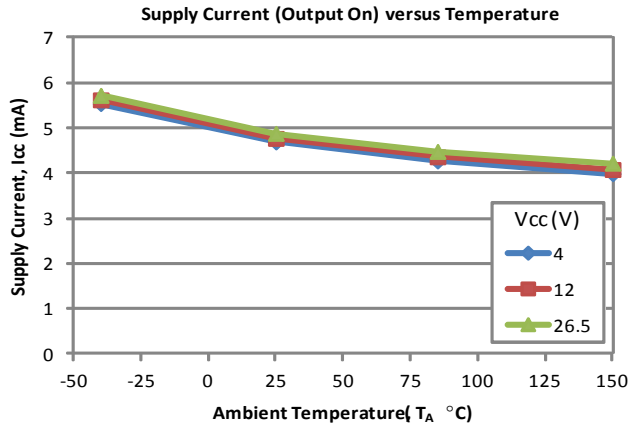
Power Derating Curves

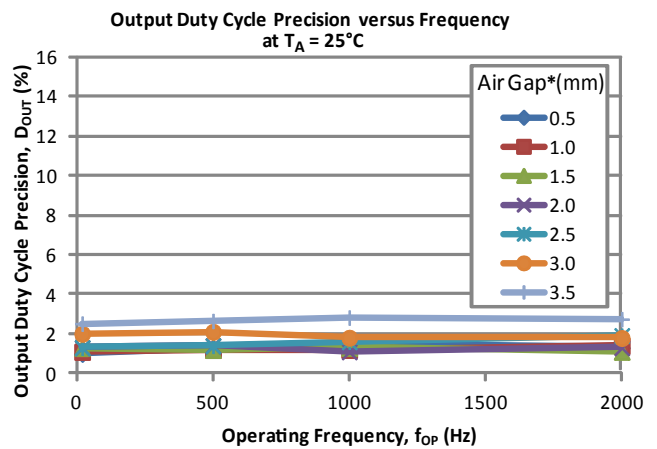
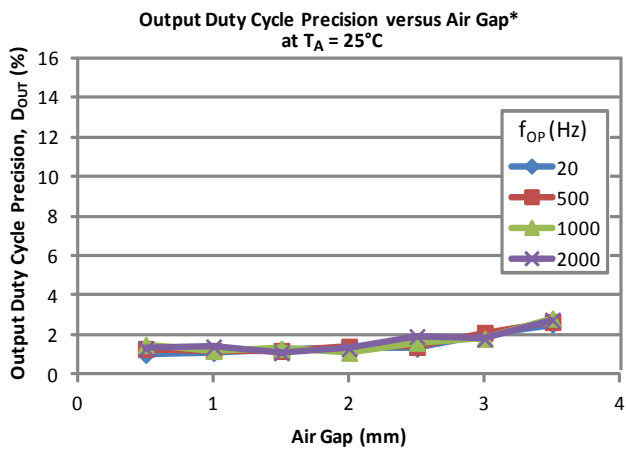
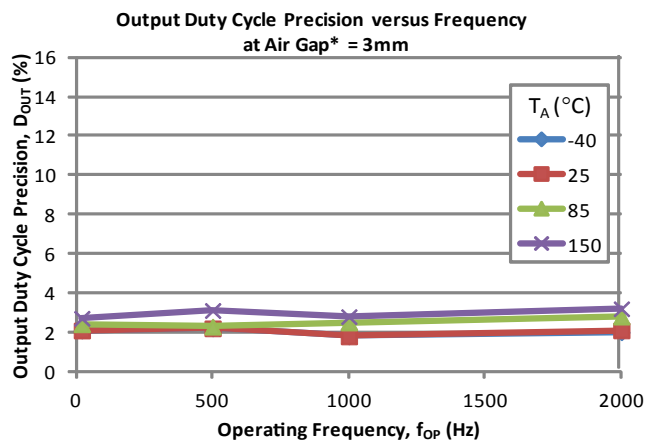
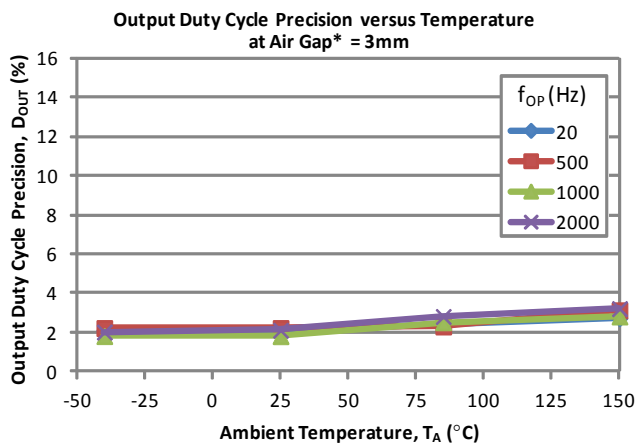
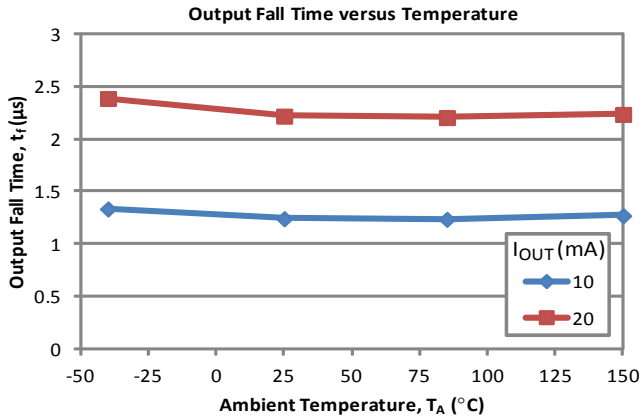


Power Dissipation versus Ambient Temperature



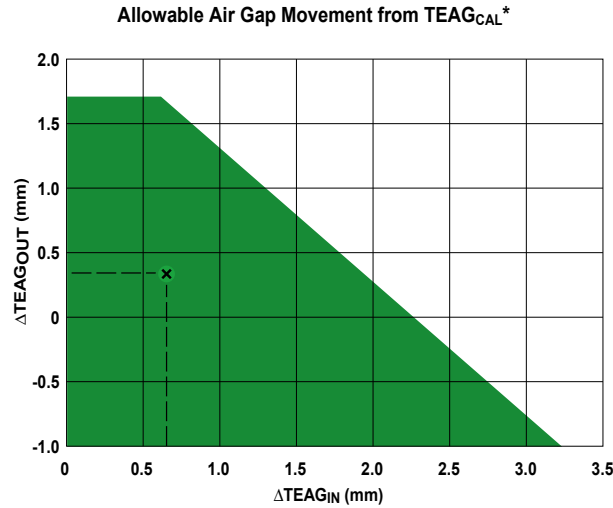
CHARACTERISTIC PERFORMANCE





\*Air gap defined as the distance between the front face of the A1469 package and the Allegro Reference Target 60-0 ring magnet.

CHARACTERISTIC ALLOWABLE AIR GAP MOVEMENT



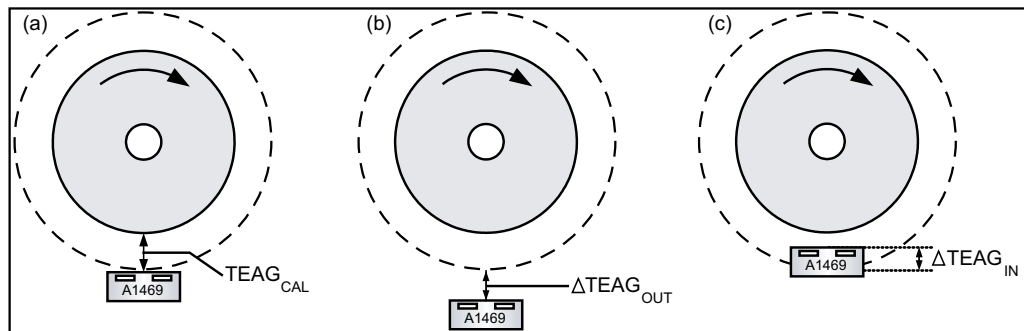
\*Data based on study performed using Allegro Reference Target 60-0 ring magnet, and applicable to ring magnet targets with similar magnetic characteristics.

The colored area in the chart above shows the region of allowable air gap movement within which the device will continue output switching. The output duty cycle is wholly dependent on the target’s magnetic signature across the air gap range of movement, and may not always be within specification throughout the entire operating region (to  $AG_{(OPmax)}$ ).

The axis parameters for the chart are defined in the drawings below. As an example, assume the case where the air gap is allowed to vary from the nominal installed air gap ( $TEAG_{CAL}$ ,

panel a) within the range defined by an increase of  $\Delta TEAG_{OUT} = 0.35$  mm (shown in panel b), and a decrease of  $\Delta TEAG_{IN} = 0.65$  mm (shown in panel c). This case is plotted with an “x” in the chart above.

Please note that after extreme cases of decrease in air gap, the device may not switch when the air gap resumes the nominal value. For example, if  $\Delta TEAG_{IN} = 2.75$  mm, the chart shows  $\Delta TEAG_{OUT} = -0.5$  mm, meaning that the device can now switch only in the air gap range of 0.5 to 2.75 mm inward from the nominal air gap.



## FUNCTIONAL DESCRIPTION

### Sensing Technology

The single-chip differential Hall effect sensor IC possesses two Hall elements, which sense the magnetic profile of the ring magnet simultaneously, but at different points (spaced at a 2.2 mm pitch), generating a differential internal analog voltage,  $V_{PROC}$ , that is processed for precise switching of the digital output signal.

The Hall IC is self-calibrating and also possesses a temperature compensated amplifier and offset compensation circuitry. Its voltage regulator provides supply noise rejection throughout the operating voltage range. Changes in temperature do not greatly affect this device due to the stable amplifier design and the offset compensation circuitry. The Hall transducers and signal processing electronics are integrated on the same silicon substrate, using a proprietary BiCMOS process.

### Target Profiling

An operating device is capable of providing digital information that is representative of the magnetic features on a rotating target. The waveform diagram shown in Figure 3 presents the automatic translation of the magnetic profile to the digital output signal of the device.

### Output Polarity

Figure 3 shows the output polarity for the orientation of target and device shown in Figure 2. The target direction of rotation shown is: perpendicular to the leads, across the face of the device, from the pin 1 side to the pin 4 side. This results in the device output switching from low to high as the leading edge of a north magnetic pole passes the device face. In this configuration, the device output voltage switches to its high polarity when a north pole is the target feature nearest to the device. If the direction of rotation is reversed, then the output polarity inverts.

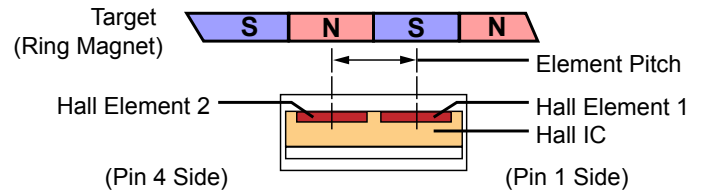


**Figure 1: Relative Motion of the Target**  
The relative motion of the target is detected by the dual Hall elements mounted on the Hall IC.

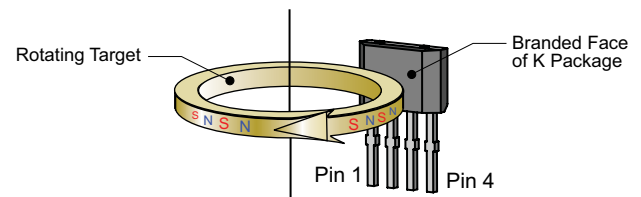


**Figure 2: Target Rotation**  
This left-to-right (pin 1 to pin 4) direction of target rotation results in a high output signal when a target north pole is nearest the face of the device (see Figure 3). A right-to-left (pin 4 to pin 1) rotation inverts the output signal polarity.



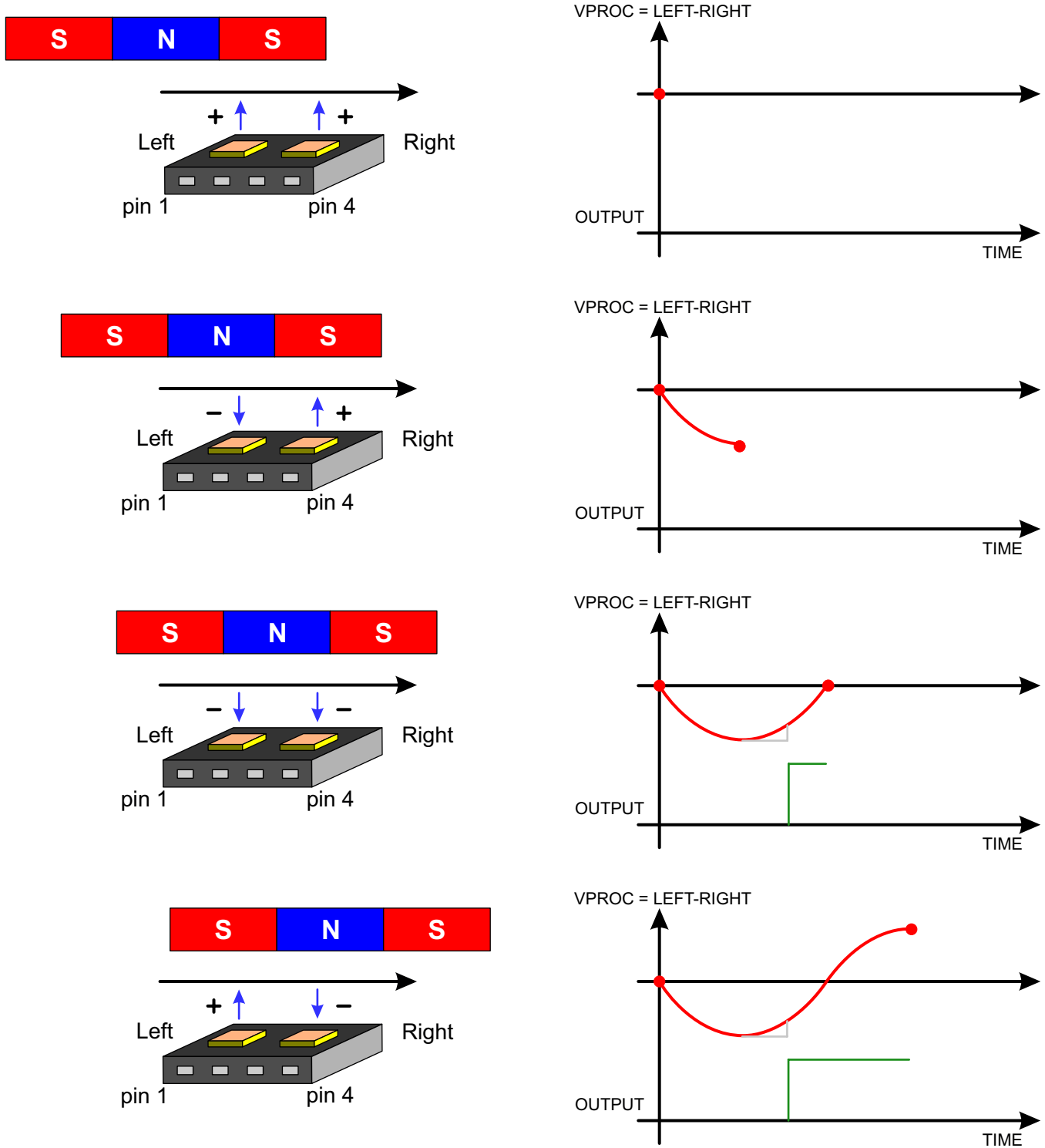


Figure 3: Output Profile of a Ring Magnet Target for the Polarity Indicated in Figure 2

**Automatic Gain Control (AGC)**

This feature allows the device to operate with an optimal internal electrical signal, regardless of the differential signal amplitude (within the  $B_{DIFF}$  and  $B_{DIFFEXT}$  specifications). During calibration, the device determines the peak-to-peak amplitude of the signal generated by the target. The gain of the device is then automatically adjusted. Figure 4 illustrates the effect of this feature. During running mode, the AGC continues to monitor the system amplitude, reducing the gain if necessary; see the Device Operation section for more details.

**Automatic Offset Adjust (AOA)**

The AOA is patented circuitry that automatically compensates for the effects of chip, magnet, and installation offsets. This circuitry is continuously active, including both during calibration mode and running mode, compensating for offset drift. Continuous operation also allows it to compensate for offsets induced by temperature variations over time.

**Digital Peak Detection**

A digital DAC tracks the internal analog voltage signal,  $V_{PROC}$ , and is used for holding the peak value of the internal analog signal. In the example shown in Figure 5, the DAC would first track up with the signal and hold the upper peak's value. When  $V_{PROC}$  drops below this peak value by  $B_{OP}$ , the device hysteresis, the output would switch and the DAC would begin tracking the signal downward toward the negative  $V_{PROC}$  peak. After the DAC acquires the negative peak, the output will again switch states when  $V_{PROC}$  is greater than the peak by the value  $B_{RP}$ . At this point, the DAC tracks up again and the cycle repeats. The digital tracking of the differential analog signal allows the device to achieve true zero-speed operation.

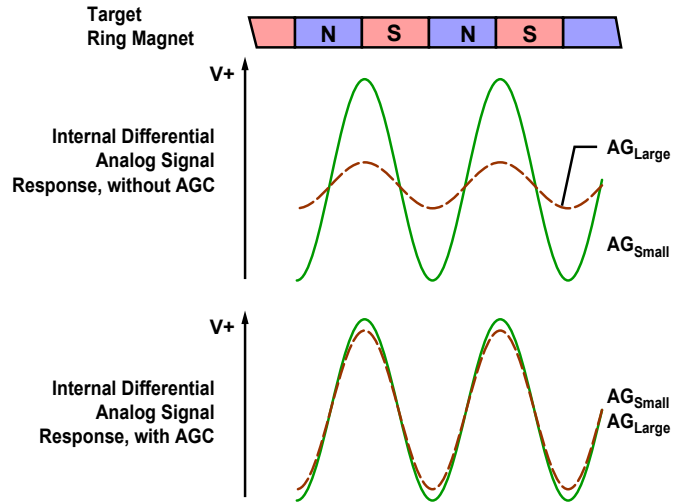


**Figure 4: Automatic Gain Control (AGC)**  
The AGC function corrects for variances in the air gap. Differences in the air gap affect the magnetic gradient, but AGC prevents that from affecting device performance, as shown in the lowest panel.

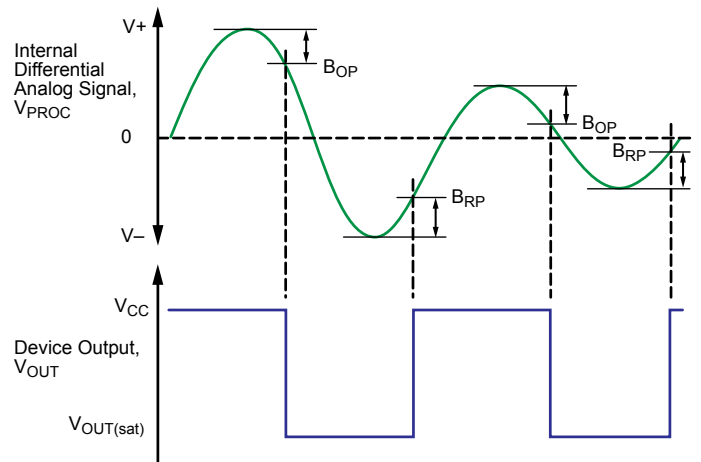


**Figure 5: Differential Signal Peaks**  
The peaks in the resulting differential signal are used to set the operate ( $B_{OP}$ ) and release ( $B_{RP}$ ) switchpoints.

### Power Supply Protection

The device contains an on-chip regulator and can operate throughout a wide  $V_{CC}$  range. For devices that must be operated from an unregulated power supply, transient protection must be added externally. For applications using a regulated line, EMI/ RFI protection may still be required. Contact Allegro for information on the circuitry required for compliance with various EMC specifications. Refer to figure 6 for an example of a basic application circuit.

### Undervoltage Lockout

When the supply voltage falls below the undervoltage lockout voltage,  $V_{CC(uv)}$ , the device enters Reset, where the output state returns to the Power-On State (POS) until sufficient  $V_{CC}$  is supplied.

### Assembly Description

This device is integrally molded into a plastic body that has been optimized for size, ease of assembly, and manufacturability. High operating temperature materials are used in all aspects of construction.

### Device Operation

Each operating mode is described in detail below.

#### POWER-ON

When power ( $V_{CC} > V_{CC(min)}$ ) is applied to the device, a short period of time is required to power the various portions of the IC. During this period, the A1469 powers-on in the high voltage state,  $V_{OUT(high)}$ , and the digital tracking DAC gets ready to

track the  $V_{PROC}$  signal. After power-on, there are conditions that could induce a change in the output state. Such an event could be caused by thermal transients, but would require a static applied magnetic field, proper signal polarity, and particular direction and magnitude of internal signal drift.

#### INITIAL OFFSET ADJUST

The device initially cancels the effects of chip, magnet, and installation offsets. After offsets have been cancelled, the device is ready to provide the first output switch. The period of time required for both Power-On and Initial Offset Adjust is defined as the Power-On Time.

#### CALIBRATION MODE

The calibration mode allows the device to automatically select the proper signal gain and continue to adjust for offsets. The AGC is active, and selects the optimal signal gain based on the amplitude of the  $V_{PROC}$  signal. Following each adjustment to the AGC DAC, the Offset DAC is also adjusted to ensure the internal analog signal is properly centered.

During this mode, the tracking DAC is active and output switching occurs, but the duty cycle is not guaranteed to be within specification.

#### RUNNING MODE

After the Initial Calibration period, CI, establishes a signal gain, the device moves to running mode. During running mode, the device tracks the input signal and gives an output edge for every peak of the signal. AOA remains active to compensate for any offset drift over time.

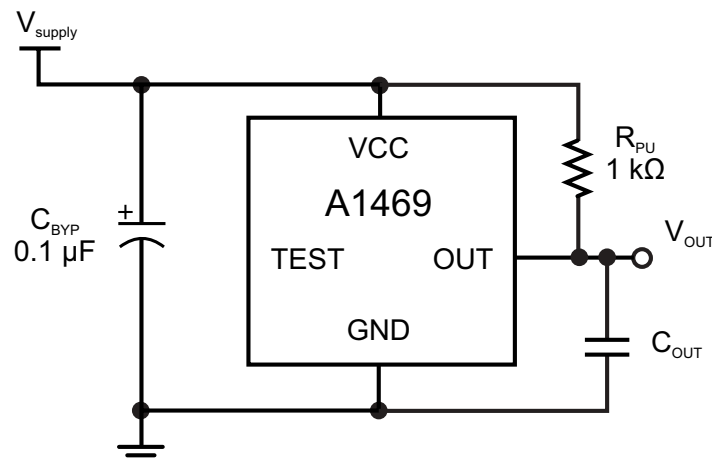
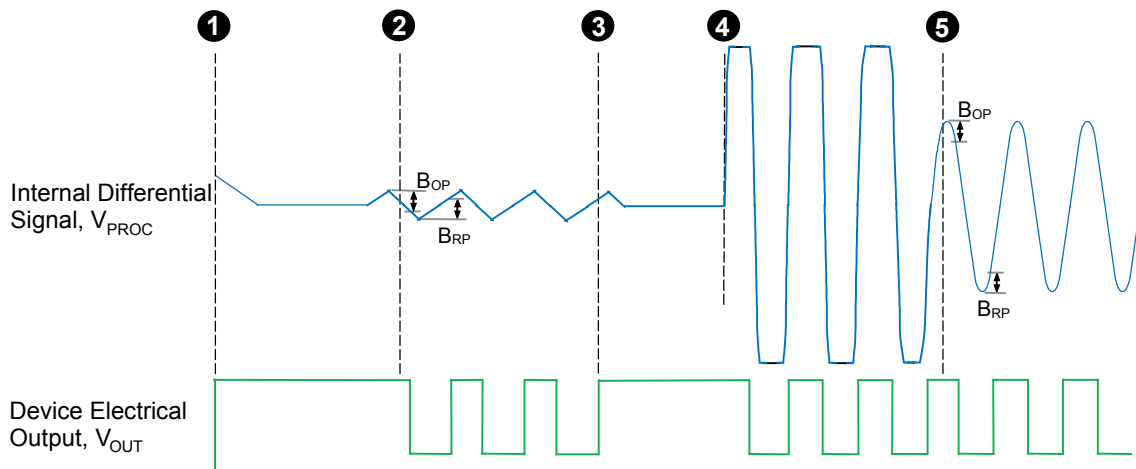


Figure 6: Typical Application Diagram

The A1469 incorporates an algorithm for adjusting the signal gain during running mode. This algorithm is designed to optimize the  $V_{PROC}$  signal amplitude in instances where the magnetic signal “seen” during the calibration period is not representative of the amplitude of the magnetic signal for the installed device air gap

(see Figure 7). Note that in this mode, the gain can be reduced but not increased, so this algorithm applies only to instances in which the magnetic signal amplitude during running is higher than that during calibration.



**Figure 7: Operation of Running Mode Gain Adjust**

- Position 1. The device is initially powered-on. Self-calibration occurs.
- Position 2. Small amplitude oscillation of the target sends an erroneously small differential signal to the device. The amplitude of  $V_{PROC}$  is greater than the switching hysteresis ( $B_{OP}$  and  $B_{RP}$ ), and the device output switches.
- Position 3. The calibration period completes on the third rising output edge, and the device enters running mode.
- Position 4. True target rotation occurs and the correct magnetic signal is generated for the installation air gap. The established signal gain is too large for the target rotational magnetic signal at the given air gap.
- Position 5. Running mode calibration corrects the signal gain to an optimal level for the installation air gap.

## Power Derating

The device must be operated below the maximum junction temperature of the device,  $T_J(\max)$ . Under certain combinations of peak conditions, reliable operation may require derating supplied power or improving the heat dissipation properties of the application. This section presents a procedure for correlating factors affecting operating  $T_J$ . (Thermal data is also available on the Allegro MicroSystems Web site.)

The Package Thermal Resistance,  $R_{\theta JA}$ , is a figure of merit summarizing the ability of the application and the device to dissipate heat from the junction (die), through all paths to the ambient air. Its primary component is the Effective Thermal Conductivity,  $K$ , of the printed circuit board, including adjacent devices and traces. Radiation from the die through the device case,  $R_{\theta JC}$ , is relatively small component of  $R_{\theta JA}$ . Ambient air temperature,  $T_A$ , and air motion are significant external factors, damped by overmolding.

The effect of varying power levels (Power Dissipation,  $P_D$ ), can be estimated. The following formulas represent the fundamental relationships used to estimate  $T_J$ , at  $P_D$ .

$$P_D = V_{IN} \times I_{IN} \quad (1)$$

$$\Delta T = P_D \times R_{\theta JA} \quad (2)$$

$$T_J = T_A + \Delta T \quad (3)$$

For example, given common conditions such as:  $T_A = 25^\circ\text{C}$ ,  $V_{CC} = 12\text{ V}$ ,  $I_{CC} = 5\text{ mA}$ , and  $R_{\theta JA} = 177\text{ }^\circ\text{C/W}$ , then:

$$P_D = V_{CC} \times I_{CC} = 12\text{ V} \times 5\text{ mA} = 60\text{ mW}$$

$$\Delta T = P_D \times R_{\theta JA} = 60\text{ mW} \times 177\text{ }^\circ\text{C/W} = 10.6^\circ\text{C}$$

$$T_J = T_A + \Delta T = 25^\circ\text{C} + 10.6^\circ\text{C} = 35.6^\circ\text{C}$$

A worst-case estimate,  $P_D(\max)$ , represents the maximum allowable power level ( $V_{CC}(\max)$ ,  $I_{CC}(\max)$ ), without exceeding  $T_J(\max)$ , at a selected  $R_{\theta JA}$  and  $T_A$ .

*Example:* Reliability for  $V_{CC}$  at  $T_A = 150^\circ\text{C}$ , package K, using minimum-K PCB.

Observe the worst-case ratings for the device, specifically:  $R_{\theta JA} = 177^\circ\text{C/W}$ ,  $T_J(\max) = 165^\circ\text{C}$ ,  $V_{CC}(\max) = 26.5\text{ V}$ , and  $I_{CC}(\max) = 7.5\text{ mA}$ .

Calculate the maximum allowable power level,  $P_D(\max)$ . First, invert equation 3:

$$\Delta T_{\max} = T_J(\max) - T_A = 165^\circ\text{C} - 150^\circ\text{C} = 15^\circ\text{C}$$

This provides the allowable increase to  $T_J$  resulting from internal power dissipation. Then, invert equation 2:

$$P_D(\max) = \Delta T_{\max} \div R_{\theta JA} = 15^\circ\text{C} \div 177\text{ }^\circ\text{C/W} = 85\text{ mW}$$

Finally, invert equation 1 with respect to voltage:

$$V_{CC}(\text{est}) = P_D(\max) \div I_{CC}(\max) = 85\text{ mW} \div 7.5\text{ mA} = 11.3\text{ V}$$

The result indicates that, at  $T_A$ , the application and device can dissipate adequate amounts of heat at voltages  $\leq V_{CC}(\text{est})$ .

Compare  $V_{CC}(\text{est})$  to  $V_{CC}(\max)$ . If  $V_{CC}(\text{est}) \leq V_{CC}(\max)$ , then reliable operation between  $V_{CC}(\text{est})$  and  $V_{CC}(\max)$  requires enhanced  $R_{\theta JA}$ . If  $V_{CC}(\text{est}) \geq V_{CC}(\max)$ , then operation between  $V_{CC}(\text{est})$  and  $V_{CC}(\max)$  is reliable under these conditions.

**PACKAGE OUTLINE DIAGRAM**

**For Reference Only - Not for Tooling Use**

(Reference DWG-9010)

Dimensions in millimeters - NOT TO SCALE

Dimensions exclusive of mold flash, gate burs, and dambar protrusions  
Exact case and lead configuration at supplier discretion within limits shown

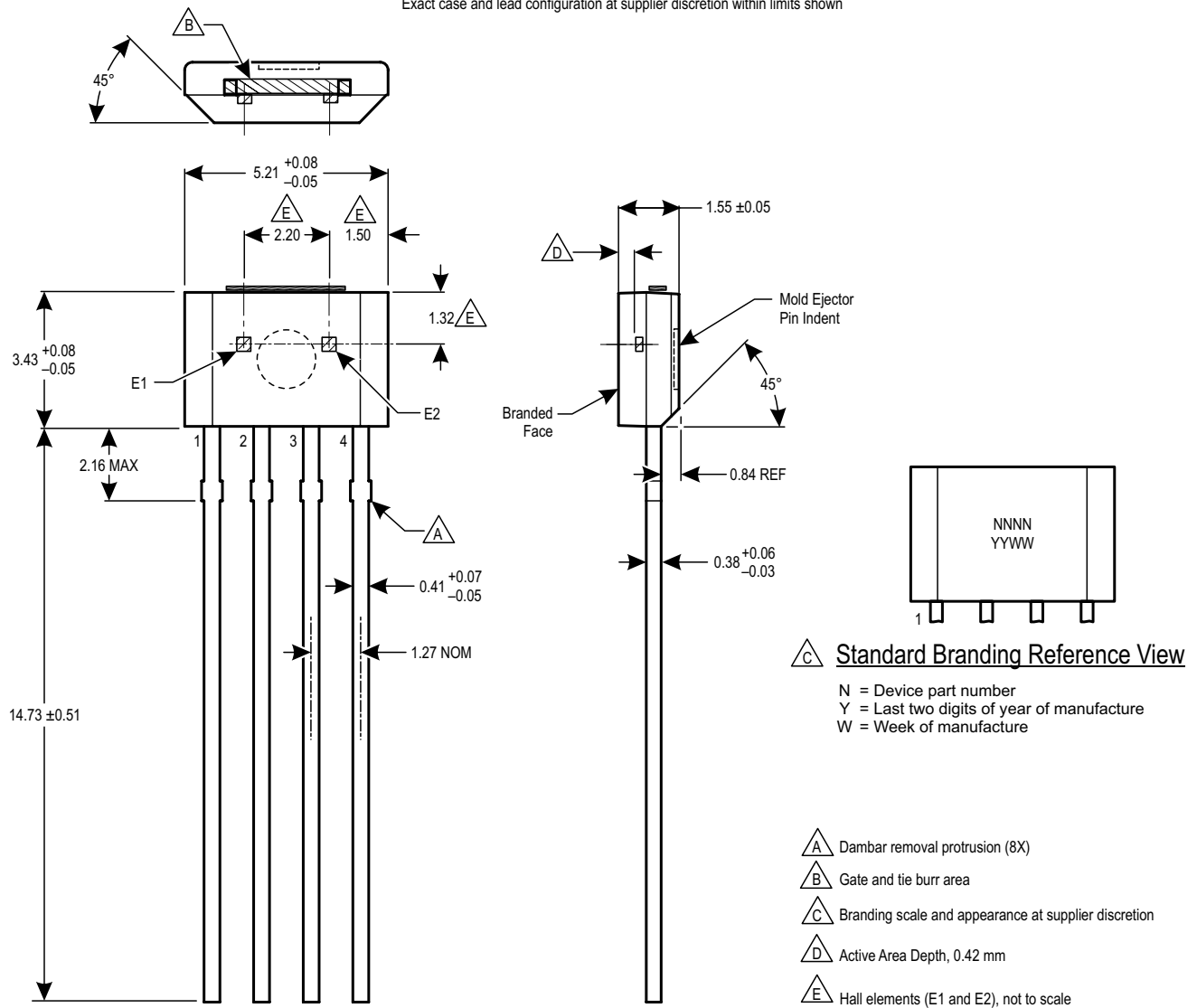


**Figure 8: Package K, 4-Pin SIP**

**Revision History**

<b>Revision</b>	<b>Current Revision Date</b>	<b>Description of Revision</b>
–	January 21, 2015	Initial Release

Copyright ©2011-2015, Allegro MicroSystems, LLC

Allegro MicroSystems, LLC reserves the right to make, from time to time, such departures from the detail specifications as may be required to permit improvements in the performance, reliability, or manufacturability of its products. Before placing an order, the user is cautioned to verify that the information being relied upon is current.

Allegro's products are not to be used in any devices or systems, including but not limited to life support devices or systems, in which a failure of Allegro's product can reasonably be expected to cause bodily harm.

The information included herein is believed to be accurate and reliable. However, Allegro MicroSystems, LLC assumes no responsibility for its use; nor for any infringement of patents or other rights of third parties which may result from its use.

For the latest version of this document, visit our website:

[www.allegromicro.com](http://www.allegromicro.com)

